Improving the Reactivity of Zerovalent Iron by Taking Advantage of Its Magnetic Memory: Implications for Arsenite Removal

ARTICLE *in* ENVIRONMENTAL SCIENCE & TECHNOLOGY · JULY 2015

Impact Factor: 5.33 · DOI: 10.1021/acs.est.5b02699 · Source: PubMed

7 AUTHORS, INCLUDING:

Zhong Shi

Tongji University

52 PUBLICATIONS **243** CITATIONS

SEE PROFILE

Xiaohong Guan

Tongji University

62 PUBLICATIONS **755** CITATIONS

SEE PROFILE

Environmental Science & Technology

Article

pubs.acs.org/est

Improving the Reactivity of Zerovalent Iron by Taking Advantage of Its Magnetic Memory: Implications for Arsenite Removal

Jinxiang Li,[†] Zhong Shi,[‡] Bin Ma,[§] Pingping Zhang,[∥] Xiao Jiang,[†] Zhongjin Xiao,[†] and Xiaohong Guan*[,†]

[†]State Key Laboratory of Pollution Control and Resources Reuse, College of Environmental Science and Engineering, and [‡]Department of Physics, Tongji University, Shanghai 200092, People's Republic of China

[§]Department of Optical Science and Engineering, Fudan University, Shanghai 200433, People's Republic of China

[∥]Institute of Functional Nano & Soft Materials (FUNSOM), Soochow University, Suzhou, Jiangsu 215123, People's Republic of China

S *Supporting Information*

ABSTRACT: Premagnetization was employed to enhance the reactivity of zerovalent iron (ZVI) toward As(III) sequestration for the first time. Compared to the pristine ZVI (Pri-ZVI), the rate of As(III) elimination by the premagnetized ZVI (Mag-ZVI) was greater over the pH_{ini} range of 4.0−9.0 and increased progressively with increasing intensity of the magnetic field for premagnetization. Mag-ZVI could keep its reactivity for a long time and showed better performance than Pri-ZVI for As(III) removal from synthetic groundwater in column tests. The Fe *K*-edge XAFS analysis for As(III)-treated ZVI samples unraveled that premagnetization promoted the transformation of ZVI to iron (hydr)oxides and shifted the corrosion products from maghemite and magnetite to lepidocrocite, which favored the arsenic sequestration. The arsenic species analysis revealed that premagnetization facilitated the oxidation of As(III) to As(V). ZVI pretreated with grinding was very different from Mag-ZVI with regard to As(III) removal, indicating that the improved reactivity of Mag-ZVI should not be associated with the physical squeezing effect of the ZVI grains during magnetization. The positive correlation between the remanence of Mag-ZVI and the rate constants of total arsenic removal indicated that the enhanced reactivity of Mag-ZVI was mainly ascribed to its magnetic memory, i.e., the remanence kept by Mag-ZVI.

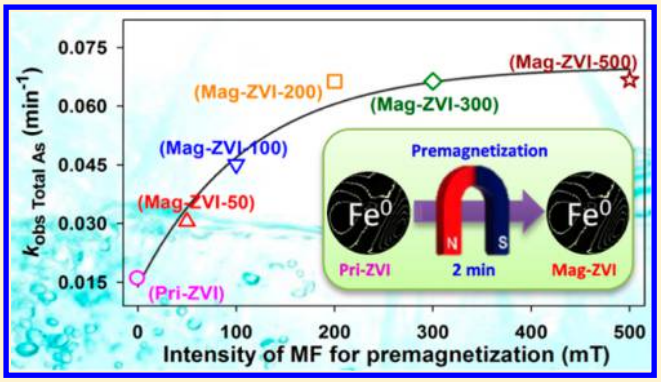

INTRODUCTION

Zerovalent iron (ZVI) has been extensively applied for the remediation/treatment of groundwater and wastewater contaminated with a wide variety of organic and inorganic pollutants,[1,2] e.g., chlorinated organics,[1,3,4] nitroaromatics,[5,6] arsenic,[2,7−10] nitrate,[11−13] chromate,[14,15] and selenite.[16] However, the granular ZVI, or iron filings, extensively examined in laboratory studies and field demonstrations,[2] has low intrinsic reactivity toward contaminants due to its inherent passive film.[17] Since the low reactivity of granular ZVI has become a major concern in further development of the ZVI-based technologies, it is highly desirable to develop methods that can significantly improve the reactivity of ZVI for environmental remediation.[17] Numerous countermeasures such as acid washing,[14] sonication,[18] H_2-reducing pretreatment,[19] electrochemical reduction,[20] fabrication of nanosized ZVI (nZVI), and synthesis of ZVI-based bimetals have been proposed to enhance the reactivity of ZVI.[21] Nevertheless, the disadvantages of these methods should be addressed, such as relatively complex procedures, extra costs, and ecotoxicity.[22]

Recently, it was reported that the application of a weak magnetic field (WMF) produced by permanent magnets could accelerate ZVI corrosion, resulting in more rapid release of Fe(II) and greater rates for Se(IV),[17,23] As(III)/As(V),[24] and Cu(II)[25] sequestration by ZVI. In the presence of a WMF, the Lorentz force gives rise to convection in the solution which narrows the diffusion layer and the magnetic field gradient force tends to move paramagnetic ions (especially Fe(II)) along the higher intensity of magnetic field at the ZVI particle surface,[25] thereby inducing nonuniform corrosion and eventually localized corrosion of ZVI. Applying a WMF generated by permanent magnets to improve the reactivity of ZVI is efficient, chemical-free, and environmentally friendly. Nevertheless, it may be a great challenge in practice to supply a WMF, generated either by permanent magnets or by electromagnets, for a large treatment unit, which would increase the costs for construction and operation, respectively. ZVI is ferromagnetic, and it becomes magnetized in an external magnetic field and remain magnetized even after the external field is removed.[26,27]

Received: June 2, 2015
Revised: July 28, 2015
Accepted: July 29, 2015
Published: July 29, 2015

DOI: 10.1021/acs.est.5b02699
Environ. Sci. Technol. 2015, 49, 10581−10588

Thus, taking advantage of the magnetic memory of ZVI, premagnetization may be employed to improve the reactivity of ZVI. However, it remains unknown whether it is possible to take advantage of the remanence of ZVI to achieve enhanced contaminant removal by ZVI.

Arsenic contamination has long been a vexing problem and poses a great health threat to millions of people.[28−31] Arsenic in aquatic environments predominantly exists in inorganic forms as arsenite (As(III)) and arsenate (As(V)).[30] Usually, As(III) is more mobile and toxic than As(V), and in turn it is more difficult to sequester.[32−34] The maximum contaminant level (MCL) for arsenic in drinking water has been lowered from 50.0 to 10.0 $\mu g\ L^{-1}$ by the World Health Organization (WHO) and U.S. Environmental Protection Agency (USEPA).[35,36] Therefore, As(III) was employed as a target contaminant to examine the influence of premagnetization on the reactivity of ZVI.

In summary, the objectives of this study were to (1) explore the feasibility of employing premagnetization to enhance the reactivity of ZVI toward As(III) removal, (2) characterize the corrosion products during As(III) sequestration by pristine ZVI (Pri-ZVI) and premagnetized ZVI (Mag-ZVI), (3) investigate the influence of initial pH values on the enhanced reactivity of ZVI toward As(III) removal by premagnetization, (4) evaluate the performance of Mag-ZVI for sequestering As(III) from synthetic groundwater in column tests, and (5) shed light on the role of premagnetization in enhancing As(III) sequestration by ZVI.

EXPERIMENTAL SECTION

Materials. All chemicals were of analytical grade and were used without further purification. All solutions were prepared with Milli-Q water, unless otherwise specified. ZVI (Alfa Aesar) used in this study was obtained from Johnson Matthey Public Co. Ltd. (London), and its basic material properties are summarized in Figure S1.

Fabrication of Mag-ZVI. The preliminary experiments showed that the optimum duration for premagnetization was 2.0 min, as shown in Figure S2. Thus, Pri-ZVI particles contained in a zipper bag were magnetized in a uniform magnetic field (MF) adjusted to different intensities (50, 100, 200, 300, and 500 mT) for 2.0 min, which were denoted as Mag-ZVI-50, Mag-ZVI-100, Mag-ZVI-200, Mag-ZVI-300, and Mag-ZVI-500, respectively. The static, uniform MF was generated by an electromagnet (Electromagnet Power Supply, model 7050), which was purchased from East Changing Technologies, Inc. (Beijing).

Bach Experiments and Column Experiments. To investigate the influence of premagnetization on As(III) removal by ZVI, batch tests were initiated by adding 0.10 g of Pri-ZVI or Mag-ZVI into a 500 mL solution (1.0 mg L^{-1} As(III) and 0.25 mM Na_2SO_4), which was freshly prepared for each batch test and mixed at 400 rpm with a mechanical stirrer. The stock solution of 1000.0 mg L^{-1} As(III) was prepared from $NaAsO_2$. The initial pH (pH_{ini}) was adjusted with NaOH and H_2SO_4, and no attempt was made to maintain a constant pH during the experiments. To differentiate the influence of premagnetization and manual grinding on the reactivity of ZVI, batch experiments were carried out to examine the performance of Gri-ZVI (ZVI after grinding) for sequestrating As(III) at pH_{ini} 4.0. The experiments were performed open to the air and at 25 °C, which was controlled with a water bath, unless otherwise specified. It should be specified that only sulfate was dosed in the batch experiments to work as the background electrolyte to minimize the coupled effects of premagnetization and coexisting ions.

Column experiments at room temperature (22 ± 1 °C) were carried out to compare the performance of Mag-ZVI-500 and Pri-ZVI in removing As(III) (150.0 $\mu g\ L^{-1}$) from synthetic groundwater (pH_{inlet} 7.5). The glass columns with an inner diameter of 2 cm, a height of 16 cm, and an internal volume of 50 mL were packed with 10.0 g of fine sand, 60.0 g of coarse sand, and 3.5 g of iron powder. The porosity of the columns was 0.24. The synthetic groundwater purged with nitrogen (DO_{inlet} = 1.2 mg L^{-1} and ORP_{inlet} = 76 ± 10 mV, with DO meaning dissolved oxygen and ORP meaning oxidation/reduction potential) passed through the columns upward at a 0.3 mL min^{-1} flow rate using a peristaltic pump, and the empty bed contact time (EBCT) was 40.0 min (Figure S3). In the synthetic groundwater, the concentrations of Na^+, HCO_3^-, SO_4^{2-}, HPO_4^{2-}, Cl^-, and $Si(OH)_4$ were 3.50, 1.00, 0.20, 0.05, 2.00, and 0.50 mM, respectively.

Chemical Analysis and Solid-Phase Characterization. Samples of batch tests and column tests were collected at given time intervals using a 10 mL syringe, filtered immediately through a 0.22 μm membrane filter, and then acidified for analysis. Concentrations of As (As(III), As(V)) and the Fe(II) concentration in solution were determined by HPLC−ICP-MS and the 1,10-phenanthroline colorimetric method using a UV−vis spectrophotometer at 510 nm,[37,38] respectively.

Morphological analysis of the As(III)-treated Mag-ZVI/Pri-ZVI samples was performed by scanning electron microscopy (SEM) using a Hitachi 4700 microscope (at 15 kV). The size distribution of the Pri-ZVI particles was examined by Bettersize 2000 (Dandong Bettersize Instruments Ltd., China). Specific surface areas of the ZVI samples were determined by nitrogen adsorption using the Brunauer−Emmett−Teller (BET) method (Micrometrics ASAP 2020). The step-scanned XRD spectrum of Pri-ZVI was collected with a Rigaku DXR-8000 computer-automated diffractometer. XRD analysis was conducted at 40 kV and 40 mA using a diffracted beam graphite monochromator and Cu radiation. The XRD patterns were collected in the 2θ range of 10−90° with a step size of 0.02° and a count time of 2 s per step.

After specific tests, the precipitates were collected on membrane filters (0.22 μm), washed with deionized water in a nitrogen-filled glovebox, then freeze-dried under vacuum, and put into zipper bags before being subjected to Fe *K*-edge and As *K*-edge X-ray absorption fine structure (XAFS) analysis. Before analysis at the beamline, the filtered solids were placed into aluminum sample holders and sealed using a Kapton tape film. Particular care was taken to minimize the beam-induced oxidation of As(III) by placing the sample stands filled with reacted ZVI samples in a nitrogen-filled glovebox for 6 h before transferring them to zippered bags in this glovebox. Negligible changes in the line shape and peak position of As *K*-edge X-ray absorption near-edge structure (XANES) spectra were observed between two scans taken for a specific sample. The XAFS spectra were recorded at room temperature using a four-channel silicon drift detector (SDD) (Bruker 5040) at beamline BL14W1 of the Shanghai Synchrotron Radiation Facility (SSRF), China. Fe and As K-edge XAFS spectra were recorded in transmission mode and fluorescence mode, respectively. The spectra were processed and analyzed by the software code Athena.[39] The oxidation states of arsenic in the solid phase were analyzed by linear combination fitting (LCF) using

DOI: 10.1021/acs.est.5b02699
Environ. Sci. Technol. 2015, 49, 10581−10588

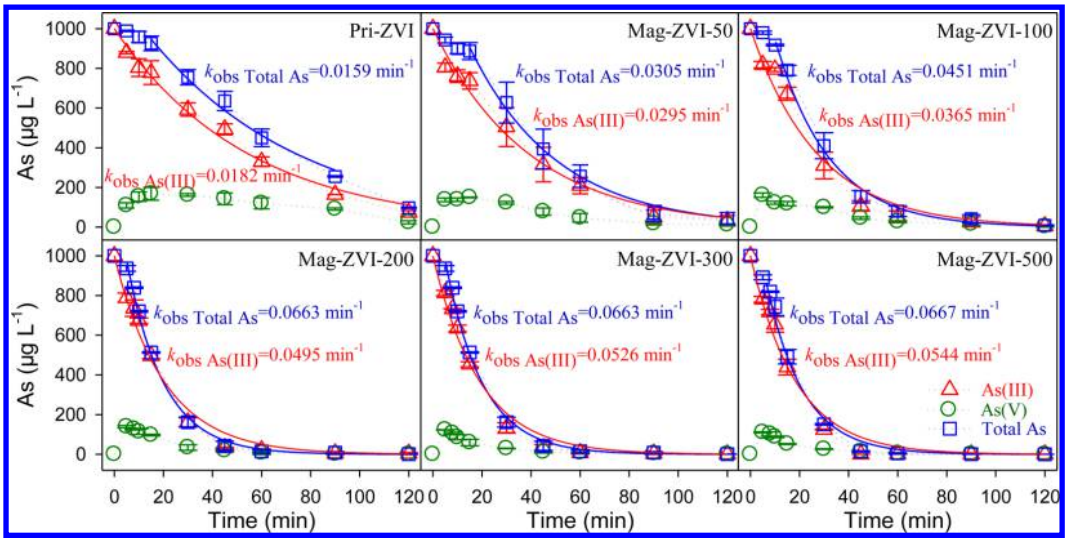

Figure 1. Depletion of total arsenic and As(III) and the evolution of As(V) (dotted lines) in the process of As(III) removal by the Pri-ZVI and Mag-ZVI fabricated in the different intensities of the MF. The solid lines are the results of simulating the kinetics of total arsenic and As(III) removal with a pseudo-first-order model. Reaction conditions: $[Fe^0]$ = 0.2 g L^{-1}, $[As(III)]_0$ = 1.0 mg L^{-1}, pH_{ini} 4.0.

reference compounds of $NaAsO_2$ (As(III)) and Na_3AsO_4 (As(V)). The major species of Fe in As-treated ZVI corrosion products were also quantified by LCF using the collection of reference materials including metallic Fe, magnetite (Fe_3O_4), maghemite (γ-Fe_2O_3), lepidocrocite (γ-FeOOH), and goethite (α-FeOOH). The magnetic hysteresis loop measurement for the pristine ZVI was carried out using a vibrating sample magnetometer (VSM; Lake Shore 7400, Lake Shore Cryotronics, Westerville, OH). To further calculate the magnetic strength distribution around the surface of the Mag-ZVI particles, Mechanical APDL (ANSYS) 14.0 was used to perform the numerical simulations.[40]

RESULTS AND DISCUSSION

Influence of Premagnetization on the Kinetics of As(III) Sequestration by ZVI. Figure 1 shows the depletion of total As and As(III), as well as the evolution of As(V) in the process of As(III) removal at pH_{ini} 4.0 by Pri-ZVI and Mag-ZVI prepared in MF with different intensities. The kinetics of total As disappearance could be roughly divided into two stages: a brief lag phase (the first 2.0−15.0 min of reaction) and thereafter a rapid stage. The lag behavior in the initial period of total As removal by ZVI, which should be mainly associated with its minor accumulation of ferric (hydr)oxides, was alleviated with increasing intensity of the MF from 0 to 500 mT for preparing the Mag-ZVI. It was found that the second stage of total As removal by Pri-ZVI and Mag-ZVI and the whole process of As(III) disappearance could be reasonably well simulated by the pseudo-first-order rate law given in eq 1,

$$\frac{d[As(III) \text{ or } As_{total}]}{dt} = -k_{obs}[As(III) \text{ or } As_{total}] \quad (1)$$

as demonstrated in Figure 1. k_{obs} is the observed pseudo-first-order rate constant (min^{-1}) of As(III) or As_{total} removal by ZVI. The sequestration rate constant was enhanced progressively from 0.0182 to 0.0544 min^{-1} for As(III) and from 0.0159 to 0.0667 min^{-1} for total As, respectively, with increasing intensity of the MF for preparing Mag-ZVI from 0 to 500 mT. Moreover, the durations necessary to achieve 99% of total As removal (equivalent to the arsenic residual of 10.0 μg L^{-1}) were 120.0, 113.5, 84.8, 82.4, and 52.2 min for Mag-ZVI-50, Mag-ZVI-100, Mag-ZVI-200, Mag-ZVI-300, and Mag-ZVI-500, respectively (Figure S4). However, only 90.2% of total As was removed by Pri-ZVI within 120.0 min. The application of premagnetization could evidently shorten the reaction time to satisfy the maximum contaminant level (MCL) (10.0 μg L^{-1}) for arsenic in drinking water.

Influence of Premagnetization on ZVI Corrosion. The rate of contaminant removal by ZVI is governed by the corrosion of ZVI,[41] which is accompanied by the release of Fe(II) and the consumption of H^+ under acidic conditions following eq 2. Thus, the variations in aqueous Fe(II) concentrations and pH in the process of As(III) sequestration by Pri-ZVI/Mag-ZVI were monitored and are shown in Figure S5. It was found that the concentration of Fe(II) increased progressively from 0 to 2.4 mg L^{-1} within 45.0 min and then remained almost constant in the process of As(III) removal by Pri-ZVI, accompanied by a slow but significant increase of the solution pH from 4.0 to 6.3 and subsequent constant pH. On the contrary, the solution pH during As(III) removal by Mag-ZVI was elevated rapidly from 4.0 to 6.3 within only 13.0 min and then dropped gradually, which was accompanied by a rapid release of Fe(II) within 15.0 min and then a gradual decrease with prolonged reaction time due to the fast oxidation of Fe(II) and release of H^+ following eqs 3−5.

$$2Fe^0 + O_2 + 2H_2O \rightarrow 2Fe^{2+} + 4OH^- \quad (2)$$

$$6Fe^{2+} + O_2 + 6H_2O \rightarrow 2Fe_3O_4 \downarrow + 12H^+ \quad (3)$$

$$4Fe^{2+} + O_2 + 6H_2O \rightarrow 4FeOOH \downarrow + 8H^+ \quad (4)$$

$$4Fe^{2+} + O_2 + 4H_2O \rightarrow 2Fe_2O_3 \downarrow + 8H^+ \quad (5)$$

The accelerated ZVI corrosion arising from premagnetization was further clarified by characterizing the As(III)-treated ZVI samples. The SEM images showed that Pri-ZVI used in this study consisted of relatively smooth spheres (Figure S1a) and became slightly coarse after reaction with As(III) for 120.0 min (Figure S6). With increasing MF intensity, the Mag-ZVI

DOI: 10.1021/acs.est.5b02699
Environ. Sci. Technol. 2015, 49, 10581−10588

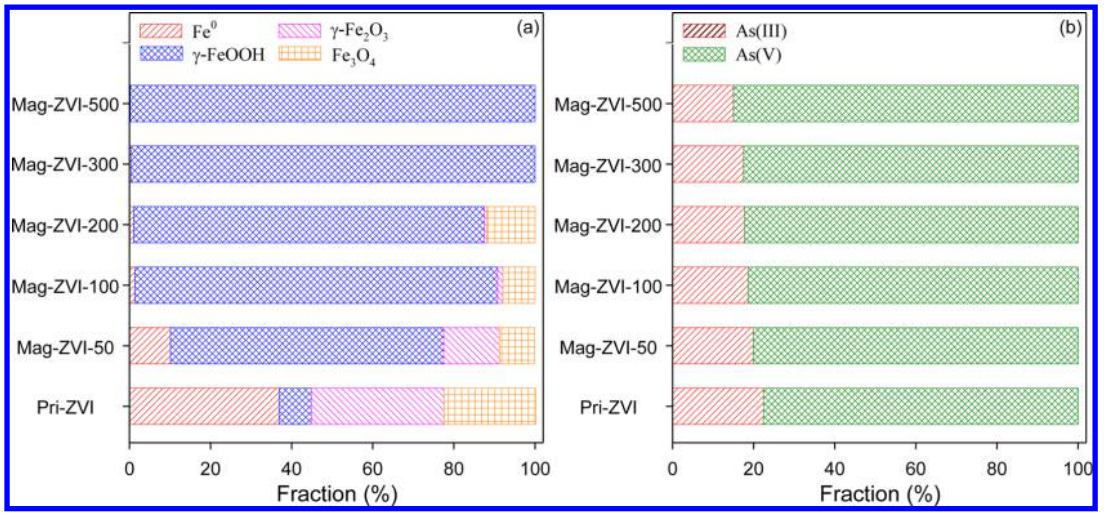

Figure 2. (a) Fractions of different Fe species in the As(III)-treated Mag-ZVI/Pri-ZVI samples, which were derived from the LCF of Fe k^3-weighted EXAFS spectra. (b) Fractions of As(III) and As(V) in the As(III)-treated Mag-ZVI/Pri-ZVI samples, which were derived from the LCF of As XANES spectra. Reaction conditions: $[Fe^0]$ = 0.2 g L^{-1}, $[As(III)]_0$ = 1.0 mg L^{-1}, pH_{ini} 4.0, reaction time 120 min.

particles became fully cracked with angular-shaped and platy structures after reaction with As(III) solution for 120.0 min, indicating more extensive corrosion with increasing MF intensity. The Fe *K*-edge XANES spectra and k^3-weighted EXAFS spectra of As(III)-treated ZVI samples and the reference materials are shown in Figure S7. Without premagnetization, the XANES and EXAFS spectra of As(III)-treated ZVI samples were analogous to those of Fe^0. With increasing intensity of the MF for fabricating Mag-ZVI, the XANES spectra of Mag-ZVI corrosion products were more analogous to those of the Fe(III) reference compounds, implying that these solids were mainly composed of nonmetallic Fe. To identify the composition of corrosion products, linear combination fitting (LCF) analysis was carried out on the basis of the Fe k^3-weighted EXAFS spectra (Figure S7b), and the corresponding fit results are summarized in Figure 2a. Premagnetization greatly enhanced the ZVI corrosion rate and lowered the fraction of Fe^0 in the As(III)-treated ZVI samples from 36.9% to 0.2−10.1%. Moreover, after ZVI was premagnetized, the major corrosion products in the As(III)-treated ZVI samples shifted from maghemite (γ-Fe_2O_3) and magnetite (Fe_3O_4) to lepidocrocite (γ-FeOOH), which has a looser and more porous structure than magnetite or maghemite, favoring the mass transport between the solid phase and aqueous phase.[42] Therefore, compared to Pri-ZVI, Mag-ZVI corroded at a much greater rate, evidenced by the faster Fe(II) release and pH variation as well as the larger fraction of iron (hydr)oxides in the As(III)-treated ZVI samples.

Influence of Premagnetization on Conversion of As(III) to As(V) by ZVI. It is well-known that As(III) can be oxidized to As(V) by $^{\bullet}OH$ radicals produced in the Fenton-like reaction under acidic conditions, following eqs 6 and 7.[43]

$$Fe^{2+} + H_2O_2 \rightarrow Fe^{3+} + {}^{\bullet}OH + OH^- \quad (7)$$

$$Fe^0 + O_2 + 2H^+ \rightarrow Fe^{2+} + H_2O_2 \quad (6)$$

Furthermore, As(III) has a low affinity for iron (hydr)oxides due to its electric neutrality, while As(V) is much more easily adsorbed or entrapped under acidic conditions.[24] Therefore, the transformation of As(III) to As(V) in the Fe^0−O_2−H_2O system is one of the key factors in understanding the As(III) removal kinetics by ZVI. The accumulation of As(V) in the process of As(III) removal by Pri-ZVI/Mag-ZVI was also determined and is shown in Figure 1. The concentration of As(V) increased to a maximum and then dropped gradually, regardless of Pri-ZVI or Mag-ZVI application. By increasing the intensity of MF for fabricating Mag-ZVI from 0 to 100 mT, As(V) was accumulated with a greater rate during the first 5.0 min of reaction, and it was also sequestrated more quickly after its concentration reached a climax. A further increase in MF intensity resulted in a drop in As(V) accumulation even in the beginning of reaction. The concentration of As(V) was dependent on both the conversion of As(III) to As(V) and the removal of As(V) by the freshly generated iron (hydr)oxides. The observed trends in As(V) accumulation with increasing MF intensity should be strongly related to the accelerated ZVI corrosion arising from premagnetization. The accelerated ZVI corrosion would speed up the transformation of As(III) to As(V) in the aqueous phase and the uptake of As(V) by iron (hydr)oxides.[24]

To further explore the influence of premagnetization on oxidation of As(III), the As speciation in the As(III)-treated ZVI samples was also analyzed with As *K*-edge XANES spectra (Figure S8). LCF analysis revealed that As in the solid phase, collected at 120 min, was predominantly present as As(V), no matter whether ZVI was premagnetized, as demonstrated in Figure 2b. The fraction of As(V) increased progressively from 77.6% to 85.0% as the intensity of the MF for preparing Mag-ZVI increased from 0 to 500 mT, indicating that premagnetization facilitated oxidation of As(III) to As(V). Combining the results of arsenic removal behavior and arsenic speciation in solution and the solid phase, it could be confirmed that the transformation of As(III) to As(V) by ZVI was improved by applying premagnetization.[24,44−46] In summary, ZVI corrosion was accelerated due to premagnetization, and Mag-ZVI prepared in an MF with greater intensity corroded at a larger rate, which favored the Fenton reaction, conversion of As(III) to As(V), and generation of iron (hydr)oxides for incorporating arsenic. Although As(III) was oxidized at a greater rate in the system with Mag-ZVI, a drop in As(V) accumulation was

DOI: 10.1021/acs.est.5b02699
Environ. Sci. Technol. 2015, 49, 10581−10588

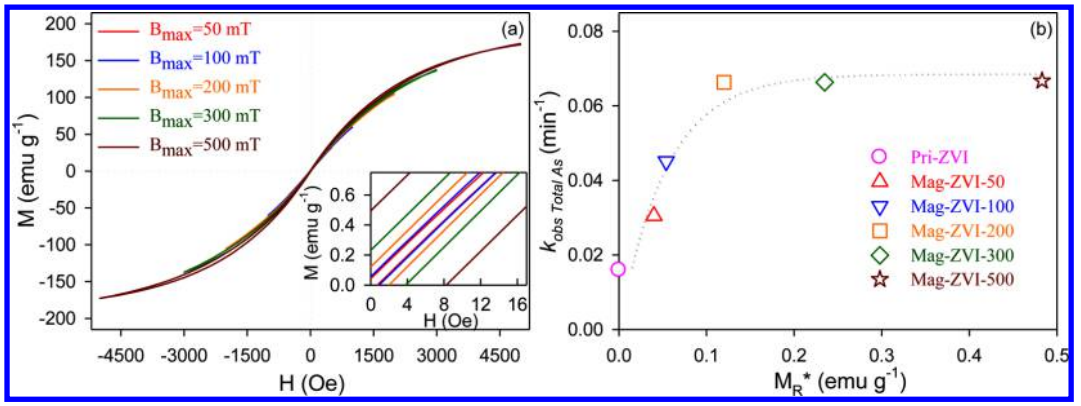

Figure 3. (a) Minor magnetic hysteresis loops of the ZVI measured with different maximal external magnetic fields at 300 K. The values of remanence are enlarged in the inset. (b) Dependence of the rate constants of total As removal by Mag-ZVI on the remanence of Mag-ZVI.

observed, as compared to its counterpart in the system with Pri-ZVI, which could be explained by the quick generation of iron (hydr)oxides.

Role of the Remanence of Mag-ZVI in As(III) Sequestration. Contaminant removal by ZVI is strongly influenced by the mass transport of the contaminants to the ZVI surface across a stagnant boundary layer.[22] The role of a WMF in contaminant removal by ZVI is to induce ZVI magnetization and generate an induced MF around the ZVI particle, which is inhomogeneous and stronger than the applied WMF. When the charged reactants move forward to the surface of ZVI or the charged products move away from the surface of ZVI, they are subject to the Lorentz force, which can give rise to convection in the solution, narrows the diffusion layer, and enhances mass transport.[47] The field gradient force tends to move paramagnetic ions (Fe^{2+}) along the higher field gradient at the ZVI particle surface, which creates localized galvanic couples and electromagnetic forces that stimulate the migration of ions, breakdown of the passive film, and eventually localized corrosion.[48]

The influence of premagnetization accelerated As(III) sequestration by ZVI, while it did not change the mechanisms of arsenic uptake, which was analogous to the influence of WMF application on Se(IV),[17,23] As(III)/As(V),[24] and Cu(II)[25] removal by ZVI reported in our previous studies. Therefore, the magnetic properties of Mag-ZVI were determined. The major magnetic hysteresis loop of ZVI obtained in a maximum flux density of 5 T (B_{max} = 5 T) was independent of the temperature, as shown in Figure S9. It was found that ZVI employed in this study exhibits a ferromagnetic behavior with a saturation magnetization value of ~220 emu g^{-1} with very small remanence, due to the multidomain state of the individual particle or of large aggregated particles (>1600 μm^2, calculated from Figure S1b).[49] To characterize the magnetic properties of Mag-ZVI (remanence of Mag-ZVI, M_R*) prepared in an MF with different intensities, a set of minor hysteresis loops of the Pri-ZVI with various amplitudes up to 500 mT (5000 Oe) were collected at 300 K (Figure 3a). As shown in Figure S10, the remanence of Mag-ZVI increases almost linearly from 0.04 to 0.48 emu g^{-1} as the B_{max} is elevated from 50 to 500 mT. Moreover, it is interesting to find that there is a strong dependence of the removal rates of As(III) by Mag-ZVI on its remanence, as illustrated in Figure 3b. Therefore, it is very possible that the premagnetization-induced enhancement in As(III) removal by ZVI is associated with the remanence of Mag-ZVI, which makes Mag-ZVI a magnet and generates an inhomogeneous magnetic field around the ZVI grain.

However, the enhancement in the reactivity of ZVI induced by premagnetization may also be associated with the physical squeezing effect of the ZVI grains during magnetization, leading to the partial breakdown of the intrinsic passive layer and thus to the improved reactivity, besides remanence. Therefore, the reactivity of ZVI pretreated with grinding (Gri-ZVI) toward As(III) removal was compared with the corresponding performances of Mag-ZVI-500 and Pri-ZVI, as shown in Figure S11. Apparently, Gri-ZVI displayed definitely different As(III) removal kinetics compared to Mag-ZVI. Gri-ZVI removed As with a greater rate during the first 10 min and a smaller rate than Mag-ZVI thereafter, which should be mainly associated with the damage of the oxide film on the Gri-ZVI particles by grinding and the following passivation from the iron oxide deposits, respectively. Additionally, BET test results showed that the specific surface area of Gri-ZVI (0.69 m^2 g^{-1}) was larger than that of Pri-ZVI (0.47 m^2 g^{-1}) and Mag-ZVI (0.47 m^2 g^{-1}). The above comparisons unraveled that the improved reactivity of Mag-ZVI compared to Pri-ZVI should be mainly associated with the remanent magnetization rather than the physical squeezing effect.

It is very difficult to quantify the MF intensity and gradient of a Mag-ZVI grain via theoretical calculation just based on the remanence of Mag-ZVI. However, the distribution of the magnetic field around a ZVI grain in a homogeneous MF can be calculated, as shown in our previous study.[23] Therefore, the performance of Mag-ZVI-500 toward As(III) removal was compared with that of Pri-ZVI in the presence of a uniform MF. It was found that the rate of total As removal at pH_{ini} 4.0 by Mag-ZVI-500 was very close to that by the pristine ZVI with the presence of a homogeneous MF of 1.0 mT (Figure S12), indicating that the distribution of the MF around a Mag-ZVI-500 grain was approximately the same as that of a Pri-ZVI particle placed in an MF with an intensity of 1.0 mT. The MF intensity distribution of a ZVI grain with a diameter of 46.2 μm in a homogeneous magnetic field of 1.0 mT was calculated with the Mechanical APDL (ANSYS) 14.0 software and is shown in Figure S13. Therefore, the maximum MF intensity around the surface of a Mag-ZVI-500 grain is closed to 2.0 mT.

Influence of Premagnetization on the Reactivity of ZVI at Various pH_{ini} Levels and on As(III) Removal from Synthetic Groundwater in a Column Test. The influences of ZVI premagnetization in an MF of 500 mT on the kinetics of total As sequestration by ZVI at various pH_{ini} levels are

DOI: 10.1021/acs.est.5b02699
Environ. Sci. Technol. 2015, 49, 10581−10588

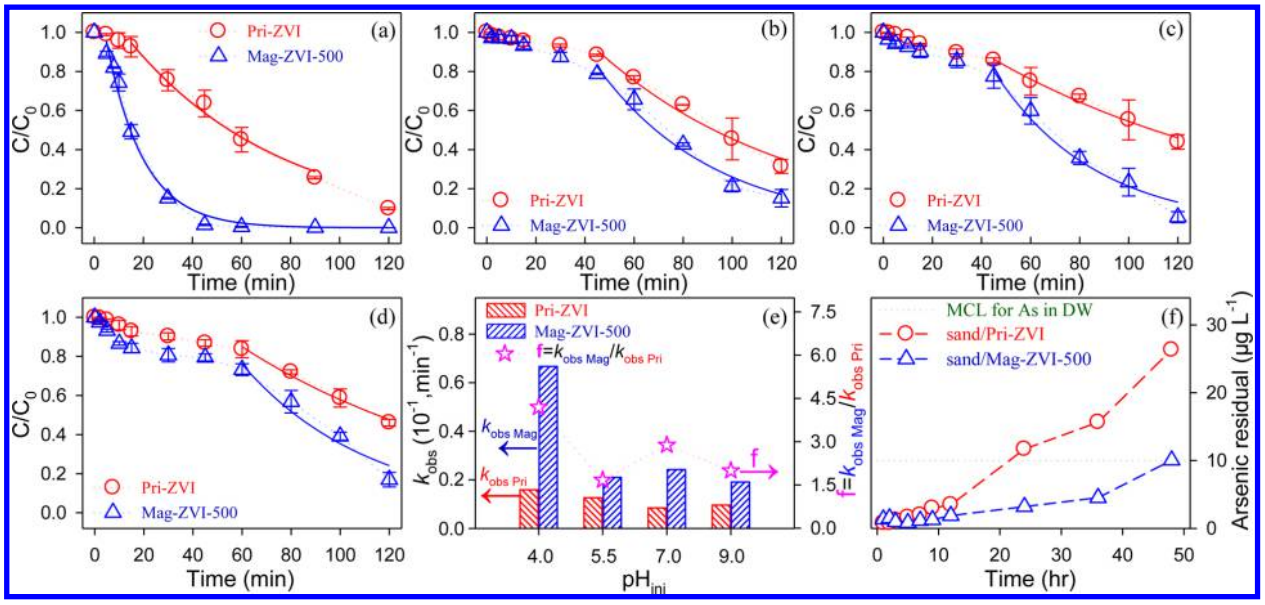

Figure 4. Kinetics of total As removal by Pri-ZVI and Mag-ZVI-500 (dotted lines) at pH_{ini} 4.0 (a), 5.5 (b), 7.0 (c), and 9.0 (d). The solid lines in (a)−(d) are the simulation results of total arsenic removal with a pseudo-first-order model. (e) Pseudo-first-order rate constants of total As removal by Pri-ZVI and Mag-ZVI-500 as well as the variations in the corresponding promotion factors ($f = k_{obs\ Mag}/k_{obs\ Pri}$). (f) Arsenic removal from a synthetic groundwater by two separate column beds packed with sand/Pri-ZVI and sand/Mag-ZVI-500, respectively. Reaction conditions for (a)−(e): $[Fe^0]$ = 0.2 g L^{-1}, $[As(III)]_0$ = 1.0 mg L^{-1}, T = 25 °C. Reaction conditions for (f): $[Fe^0]$ = 70 g L^{-1}, m_{Fe}:m_{sand} = 1:20, $[As(III)]_{inlet}$ = 150.0 μg L^{-1}, DO = 1.2 mg L^{-1}, pH_{inlet} 7.5, ORP_{inlet} = 76 ± 10 mV, V_{column} = 50.0 mL, Q = 0.3 mL min^{-1}, empty bed contact time (EBCT) of 40 min.

demonstrated in Figure 4a−e. Manifestly, the application of premagnetization enhanced As removal by ZVI over the pH_{ini} range of 4.0−9.0, and the enhancement was most significant at pH_{ini} 4.0. Total As removal by Pri-ZVI at pH_{ini} 4.0−9.0 can be divided into two stages, a lag period followed by a rapid removal period. With increasing pH_{ini} from 4.0 to 9.0, the lag period of total As removal by Pri-ZVI increased from 15.0 to 60.0 min. Premagnetization at 500 mT greatly shortened the lag period at pH_{ini} 4.0, while it did not decrease the lag period at pH_{ini} 5.5−9.0. The second stage of total As removal by Pri-ZVI and Mag-ZVI-500 was simulated with a pseudo-first-order model. It was found that the rate constants of total As removal by ZVI were increased appreciably from 0.0159 to 0.0667 min^{-1} at pH_{ini} 4.0, from 0.0126 to 0.0210 min^{-1} at pH_{ini} 5.5, from 0.0084 to 0.0242 min^{-1} at pH_{ini} 7.0, and from 0.0096 to 0.0191 min^{-1} at pH_{ini} 9.0 with the application of premagnetization. The corresponding promotion factors ($f = k_{obs\ Mag}/k_{obs\ Pri}$) for As sequestration by premagnetization varied from 1.7 to 4.2 (Figure 4e). The scenarios of Figure 4a−d were consistent with the variations of pH during As(III) removal (Figure S14), which confirmed that the premagnetization enhanced the reactivity of ZVI toward As(III) removal.

The influence of premagnetization on the reactivity of ZVI for sequestering As(III) from the synthetic groundwater was investigated with two separate columns filled with sand/Pri-ZVI and sand/Mag-ZVI under oxygen-limiting conditions, respectively, as depicted in Figure 4f. The residual arsenic in the effluent of the column filled with sand/Pri-ZVI violated the MCL for arsenic (10.0 μg L^{-1}) in drinking water at ∼22 h, whereas the effluent of the column filled with sand/Mag-ZVI-500 did not exceed the acceptable level until being operated for ∼48 h under otherwise identical conditions. Additionally, the solution pH from the column (filled with sand/Mag-ZVI-500) outlet increased during the first 5.0 h in a more dynamic and more variable manner than that from the column filled with sand/Pri-ZVI and then remained almost constant (Figure S15). It should be specified that the pH elevation during the initial period should be mainly ascribed to the consumption of H^+ due to ZVI corrosion. Moreover, the influence of Mag-ZVI's long-term storage on As removal by Mag-ZVI-500 in 60 min was evaluated, as shown in Figure S16. With increasing storage time of Mag-ZVI-500 from 0 to 30 days after it was fabricated in an MF, the corresponding As removal in 60.0 min dropped slightly from 99.5% to 87.2%, implying that Mag-ZVI could keep its reactivity for a long time.

Environmental Implications. This study offers an innovative, effective, simple, chemical-free method for improving the reactivity of ZVI toward As(III) removal by premagnetizing it in a homogeneous electromagnetic field. By increasing intensity of the MF for preparing Mag-ZVI, the rates of As(III) sequestration by Mag-ZVI were progressively enhanced, which was ascribed to the magnetic memory of ZVI, i.e., the remanence kept by ZVI. Premagnetization induces an influence on the reactivity of ZVI toward contaminant sequestration similar to that of WMF application, but it is superior to WMF application in several aspects. First, ZVI premagnetization is much more easily implemented in real practice than WMF application around a large treatment unit. Second, aggregation of ZVI can be avoided when premagnetization is employed to improve the reactivity of ZVI, while one obstacle of WMF application is ZVI aggregation, especially in an MF with an intensity greater than 3.0 mT. Mag-ZVI holds higher reactivity than Pri-ZVI and is expected to remove other contaminants, e.g., As(V), Se(IV), Cu(II), and Cr(VI), besides As(III), with greater rate constants than Pro-ZVI, which will be examined in our future study. Employing premagnetization to improve the reactivity of ZVI will definitely count much in the field of ZVI-based technology since this method is much more advantageous than most of the methods reported in the literature. However, more efforts should be taken to evaluate this technology more thoroughly, and the promoting effects of premagnetization on the reactivity of ZVI under neutral and

DOI: 10.1021/acs.est.5b02699
Environ. Sci. Technol. 2015, 49, 10581−10588

alkaline conditions should be amplified before it can be used widely.

■ ASSOCIATED CONTENT

Supporting Information

The Supporting Information is available free of charge on the ACS Publications website at DOI: 10.1021/acs.est.5b02699.

SEM image, particle size distribution, and XRD pattern of the pristine ZVI, influence of the pristine premagnetization duration on Mag-ZVI-500 performance, diagram of the column-testing apparatus, time to achieve total As removal (99%), variation of dissolved Fe(II) and pH during As(III) removal, SEM images of Pri-ZVI/Mag-ZVI, XANES and EXAFS spectra of Pri-ZVI/Mag-ZVI, XANES spectra of premagnetized ZVI, magnetic hysteresis loops of Pri-ZVI, correlation of Mag-ZVI remanence with the field amplitude, Mag-ZVI, Pri-ZVI, and Gri-ZVI performances, simulation of the arsenic removal kinetics, magnetic field strength distribution of the plane parallel to the applied magnetic field, and influence of long-term storage on As removal by Mag-ZVI-500 (PDF)

■ AUTHOR INFORMATION

Corresponding Author

*E-mail: guanxh@tongji.edu.cn; phone: +86-21-65980956.

Notes

The authors declare no competing financial interest.

■ ACKNOWLEDGMENTS

This work was supported by the National Natural Science Foundation of China (Grants 21277095 and 51478329), the Specialized Research Fund for the Doctoral Program of Higher Education (Grant 20130072110026), and Tongji University Open Funding for Materials Characterization. We thank Beamline BL14W1 (Shanghai Synchrotron Radiation Facility) for providing the beam time and Zhenghuan Zhao for his help with the measurements of magnetic hysteresis loops.

■ REFERENCES

(1) Scherer, M. M.; Balko, B. A.; Gallagher, D. A.; Tratnyek, P. G. Correlation analysis of rate constants for dechlorination by zero-valent iron. *Environ. Sci. Technol.* **1998**, *32* (19), 3026−3033.

(2) Obiri-Nyarko, F.; Grajales-Mesa, S. J.; Malina, G. An overview of permeable reactive barriers for in situ sustainable groundwater remediation. *Chemosphere* **2014**, *111*, 243−59.

(3) Cheng, S. F.; Wu, S. C. Feasibility of using metals to remediate water containing TCE. *Chemosphere* **2001**, *43* (8), 1023−1028.

(4) Johnson, T. L.; Scherer, M. M.; Tratnyek, P. G. Kinetics of halogenated organic compound degradation by iron metal. *Environ. Sci. Technol.* **1996**, *30* (8), 2634−2640.

(5) Agrawal, A.; Tratnyek, P. G. Reduction of nitro aromatic compounds by zero-valent iron metal. *Environ. Sci. Technol.* **1996**, *30* (1), 153−160.

(6) Scherer, M. M.; Johnson, K. M.; Westall, J. C.; Tratnyek, P. G. Mass transport effects on the kinetics of nitrobenzene reduction by iron metal. *Environ. Sci. Technol.* **2001**, *35* (13), 2804−2811.

(7) Su, C. M.; Puls, R. W. Arsenate and arsenite removal by zerovalent iron: Effects of phosphate, silicate, carbonate, borate, sulfate, chromate, molybdate, and nitrate, relative to chloride. *Environ. Sci. Technol.* **2001**, *35* (22), 4562−4568.

(8) Leupin, O. X.; Hug, S. J.; Badruzzaman, A. B. M. Arsenic removal from Bangladesh tube well water with filter columns containing zerovalent iron filings and sand. *Environ. Sci. Technol.* **2005**, *39* (20), 8032−8037.

(9) Du, Q.; Zhang, S. J.; Pan, B. C.; Lv, L.; Zhang, W. M.; Zhang, Q. X. Bifunctional resin-ZVI composites for effective removal of arsenite through simultaneous adsorption and oxidation. *Water Res.* **2013**, *47* (16), 6064−6074.

(10) Yan, W. L.; Ramos, M. A. V.; Koel, B. E.; Zhang, W. X. As(III) Sequestration by Iron Nanoparticles: Study of Solid-Phase Redox Transformations with X-ray Photoelectron Spectroscopy. *J. Phys. Chem. C* **2012**, *116* (9), 5303−5311.

(11) Huang, C. P.; Wang, H. W.; Chiu, P. C. Nitrate reduction by metallic iron. *Water Res.* **1998**, *32* (8), 2257−2264.

(12) Chi, I.; Zhang, S. T.; Lu, X.; Dong, L. H.; Yao, S. L. Chemical reduction of nitrate by metallic iron. *J. Water Supply: Res. Technol.—Aqua* **2004**, *53* (1), 37−41.

(13) Liou, Y. H.; Lo, S. L.; Lin, C. J.; Kuan, W. H.; Weng, S. C. Chemical reduction of an unbuffered nitrate solution using catalyzed and uncatalyzed nanoscale iron particles. *J. Hazard. Mater.* **2005**, *127* (1−3), 102−110.

(14) Lai, K. C. K.; Lo, I. M. C. Removal of chromium (VI) by acid-washed zero-valent iron under various groundwater geochemistry conditions. *Environ. Sci. Technol.* **2008**, *42* (4), 1238−1244.

(15) Lu, X.; Li, M.; Tang, C. M.; Feng, C. P.; Liu, X. Electrochemical depassivation for recovering Fe-0 reactivity by Cr(VI) removal with a permeable reactive barrier system. *J. Hazard. Mater.* **2012**, *213-214*, 355−360.

(16) Liang, L.; Yang, W.; Guan, X.; Li, J.; Xu, Z.; Wu, J.; Huang, Y.; Zhang, X. Kinetics and mechanisms of pH-dependent selenite removal by zero valent iron. *Water Res.* **2013**, *47* (15), 5846−55.

(17) Liang, L.; Sun, W.; Guan, X.; Huang, Y.; Choi, W.; Bao, H.; Li, L.; Jiang, Z. Weak magnetic field significantly enhances selenite removal kinetics by zero valent iron. *Water Res.* **2014**, *49*, 371−80.

(18) Geiger, C. L.; Clausen, C. A.; Reinhart, D. R.; Clausen, C. M.; Ruiz, N.; Quinn, J. Using ultrasound for restoring iron activity in permeable reactive barriers. *Acs. Sym. Ser.* **2003**, *837*, 286−303.

(19) Liou, Y. H.; Lo, S. L.; Lin, C. J.; Kuan, W. H.; Weng, S. C. Effects of iron surface pretreatment on kinetics of aqueous nitrate reduction. *J. Hazard. Mater.* **2005**, *126* (1−3), 189−194.

(20) Chen, L.; Jin, S.; Fallgren, P. H.; Swoboda-Colberg, N. G.; Liu, F.; Colberg, P. J. S. Electrochemical depassivation of zero-valent iron for trichloroethene reduction. *J. Hazard. Mater.* **2012**, *239-240*, 265−269.

(21) Zhu, B. W.; Lim, T. T. Catalytic reduction of Chlorobenzenes with Pd/Fe nanoparticles: reactive sites, catalyst stability, particle aging, and regeneration. *Environ. Sci. Technol.* **2007**, *41* (21), 7523−7529.

(22) Guan, X. H.; Sun, Y. K.; Qin, H. J.; Li, J. X.; Lo, I. M. C.; He, D.; Dong, H. R. The Limitations of Applying Zero-Valent Iron Technology in Contaminants Sequestration and the Corresponding Countermeasures: The Development in Zero-Valent Iron Technology in the Last Two Decades (1994−2014). *Water Res.* **2015**, *75*, 224−248.

(23) Liang, L. P.; Guan, X. H.; Shi, Z.; Li, J. L.; Wu, Y. N.; Tratnyek, P. G. Coupled Effects of Aging and Weak Magnetic Fields on Sequestration of Selenite by Zero-Valent Iron. *Environ. Sci. Technol.* **2014**, *48* (11), 6326−6334.

(24) Sun, Y. K.; Guan, X. H.; Wang, J. M.; Meng, X. G.; Xu, C. H.; Zhou, G. M. Effect of Weak Magnetic Field on Arsenate and Arsenite Removal from Water by Zerovalent Iron: An XAFS Investigation. *Environ. Sci. Technol.* **2014**, *48* (12), 6850−6858.

(25) Jiang, X.; Qiao, J. L.; Lo, I. M. C.; Wang, L.; Guan, X. H.; Lu, Z. P.; Zhou, G. M.; Xu, C. H. Enhanced paramagnetic Cu^{2+} ions removal by coupling a weak magnetic field with zero valent iron. *J. Hazard. Mater.* **2015**, *283*, 880−887.

(26) Aziz, F.; Pandey, P.; Chandra, M.; Khare, A.; Rana, D. S.; Mavani, K. R. Surface morphology, ferromagnetic domains and magnetic anisotropy in $BaFeO_{3-\delta}$ thin films: Correlated structure and magnetism. *J. Magn. Magn. Mater.* **2014**, *356*, 98−102.

DOI: 10.1021/acs.est.5b02699
Environ. Sci. Technol. 2015, 49, 10581−10588

(27) Ghosh, N.; Mandal, B. K.; Mohan Kumar, K. Magnetic memory effect in chelated zero valent iron nanoparticles. *J. Magn. Magn. Mater.* **2012**, *324* (22), 3839−3841.
(28) Rodriguez-Lado, L.; Sun, G. F.; Berg, M.; Zhang, Q.; Xue, H. B.; Zheng, Q. M.; Johnson, C. A. Groundwater Arsenic Contamination Throughout China. *Science* **2013**, *341* (6148), 866−868.
(29) Sun, Y. K.; Zhou, G. M.; Xiong, X. M.; Guan, X. H.; Li, L. N.; Bao, H. L. Enhanced arsenite removal from water by $Ti(SO_4)_2$ coagulation. *Water Res.* **2013**, *47* (13), 4340−4348.
(30) Clancy, T. M.; Hayes, K. F.; Raskin, L. Arsenic Waste Management: A Critical Review of Testing and Disposal of Arsenic-Bearing Solid Wastes Generated during Arsenic Removal from Drinking Water. *Environ. Sci. Technol.* **2013**, *47* (19), 10799−10812.
(31) Nickson, R.; McArthur, J.; Burgess, W.; Ahmed, K. M.; Ravenscroft, P.; Rahmanñ, M. Arsenic poisoning of Bangladesh groundwater. *Nature* **1998**, *395* (6700), 338−338.
(32) Shen, S. W.; Li, X. F.; Cullen, W. R.; Weinfeld, M.; Le, X. C. Arsenic Binding to Proteins. *Chem. Rev.* **2013**, *113* (10), 7769−7792.
(33) Dixit, S.; Hering, J. G. Comparison of arsenic(V) and arsenic(III) sorption onto iron oxide minerals: Implications for arsenic mobility. *Environ. Sci. Technol.* **2003**, *37* (18), 4182−4189.
(34) Sharma, V. K.; Sohn, M. Aquatic arsenic: Toxicity, speciation, transformations, and remediation. *Environ. Int.* **2009**, *35* (4), 743−759.
(35) Guan, X. H.; Ma, J.; Dong, H. R.; Jiang, L. Removal of arsenic from water: Effect of calcium ions on As(III) removal in the $KMnO_4$-Fe(II) process. *Water Res.* **2009**, *43* (20), 5119−5128.
(36) Office of Solid Waste and Emergency Response, United States Environmental Protection Agency. *Arsenic Treatment Technologies for Soil, Waste, And Water*; U.S. Environmental Protection Agency: Washington, DC, 2002.
(37) Chen, Z. L.; Akter, K. F.; Rahman, M. M.; Naidu, R. The separation of arsenic species in soils and plant tissues by anion-exchange chromatography with inductively coupled mass spectrometry using various mobile phases. *Microchem. J.* **2008**, *89* (1), 20−28.
(38) Sun, Y. K.; Xiong, X. M.; Zhou, G. M.; Li, C. Y.; Guan, X. H. Removal of arsenate from water by coagulation with in situ formed versus pre-formed Fe(III). *Sep. Purif. Technol.* **2013**, *115*, 198−204.
(39) Ravel, B.; Newville, M. ATHENA, ARTEMIS, HEPHAESTUS: data analysis for X-ray absorption spectroscopy using IFEFFIT. *J. Synchrotron Radiat.* **2005**, *12*, 537−541.
(40) Farinon, S. Magnet design and optimization: The INFN-Genova experience using ANSYS. *Cryogenics* **2007**, *47* (11−12), 577−582.
(41) Triszcz, J. M.; Porta, A.; Einschlag, F. S. G. Effect of operating conditions on iron corrosion rates in zero-valent iron systems for arsenic removal. *Chem. Eng. J.* **2009**, *150* (2−3), 431−439.
(42) Neumann, A.; Kaegi, R.; Voegelin, A.; Hussam, A.; Munir, A. K.; Hug, S. J. Arsenic removal with composite iron matrix filters in Bangladesh: a field and laboratory study. *Environ. Sci. Technol.* **2013**, *47* (9), 4544−54.
(43) Katsoyiannis, I. A.; Ruettimann, T.; Hug, S. J. pH dependence of Fenton reagent generation and As(III) oxidation and removal by corrosion of zero valent iron in aerated water. *Environ. Sci. Technol.* **2008**, *42* (19), 7424−7430.
(44) Pang, S. Y.; Jiang, J.; Ma, J.; Pang, S. Y.; Ouyang, F. New Insight into the Oxidation of Arsenite by the Reaction of Zerovalent Iron and Oxygen. Comment on ″pH Dependence of Fenton Reagent Generation and As(III) Oxidation and Removal by Corrosion of Zero Valent Iron in Aerated Water″. *Environ. Sci. Technol.* **2009**, *43* (10), 3978−3979.
(45) Noubactep, C. Comment on ″pH Dependence of Fenton Reagent Generation and As(III) Oxidation and Removal by Corrosion of Zero Valent Iron in Aerated Water″. *Environ. Sci. Technol.* **2009**, *43* (1), 233−233.
(46) Ona-Nguema, G.; Morin, G.; Wang, Y. H.; Foster, A. L.; Juillot, F.; Calas, G.; Brown, G. E. XANES Evidence for Rapid Arsenic(III) Oxidation at Magnetite and Ferrihydrite Surfaces by Dissolved O_2 via Fe^{2+}-Mediated Reactions. *Environ. Sci. Technol.* **2010**, *44* (14), 5416−5422.
(47) Lioubashevski, O.; Katz, E.; Willner, I. Magnetic field effects on electrochemical processes: A theoretical hydrodynamic model. *J. Phys. Chem. B* **2004**, *108* (18), 5778−5784.
(48) Sueptitz, R.; Tschulik, K.; Uhlemann, M.; Schultz, L.; Gebert, A. Effect of high gradient magnetic fields on the anodic behaviour and localized corrosion of iron in sulphuric acid solutions. *Corros. Sci.* **2011**, *53* (10), 3222−3230.
(49) Batista, L.; Rabe, U.; Hirsekorn, S. Determination of the easy axes of small ferromagnetic precipitates in a bulk material by combined magnetic force microscopy and electron backscatter diffraction techniques. *Ultramicroscopy* **2014**, *146*, 17−26.

DOI: 10.1021/acs.est.5b02699
Environ. Sci. Technol. 2015, 49, 10581−10588